Constrained nonlinear predictive control for maximizing production in polymerization processes ⋆

Mazen Alamir [a], Nida Sheibat-Othman [b], Sami Othman [b],

[a] *Laboratoire d'Automatique de Grenoble (LAG). CNRS-UMR5528. BP 46, Domaine Universitaire, 38400 Saint Martin d'Hères. France*

[b] *Laboratoire d'Automatique et de Génie des Procédés (LAGEP) Bât. 308G 43, Bd du 11 Nov. 1918 69622 Villeurbanne Cedex, France.*

Abstract

In this paper, a new constrained nonlinear predictive control scheme is proposed for maximizing the production in polymerization processes. The key features of the proposed feedback strategy are its ability to rigorously handle the process constraints (input saturation, maximum allowed heat production, maximal temperature values and rate of change) as well as its real time implementability due to the low dimensional control parametrization being used. Simulations are proposed to show the efficiency of the proposed feedback as well as its robustness to model uncertainties.The controller performance is also validated experimentally on a laboratory scale reactor to control the emulsion polymerization of styrene.

Key words: Emulsion polymerization; Nonlinear predictive control; Constrained control; maximal production.

1 Introduction

Optimizing the process productivity is of great interest in emulsion polymerizations. Being rapid, exothermic and sensitive to impurities, these processes may cause a runaway reaction and require therefore to be online monitored and controlled in order to ensure the process security and minimize the process time.

⋆ This paper was not presented at any IFAC meeting. Corresponding author Nida Sheibat-Othman, Bât. 308G 43, Bd du 11 Nov. 1918 69622 Villeurbanne Cedex Tél. : 04.72.43.18.50 Fax: 04.72.43.16.99 e-mail: nida.othman@lagep.cpe.fr

Email addresses: mazen.alamir@inpg.fr (Mazen Alamir), nida.othman@lagep.cpe.fr (Nida Sheibat-Othman), othman@lagep.cpe.fr (Sami Othman).

In emulsion polymerization, the reaction rate is related to the reaction temperature and to the concentrations of monomer and radicals in the polymer particles . The concentration of monomer in the polymer particles is proportional to the reaction rate. Controlling this parameter can be done by manipulating the feed rate of monomer. On the contrary, the relation between the concentration of radicals in the polymer particles and the initiator feed is not always evident. Therefore, the initiator feed rate cannot be used to control the reaction rate. In contrast, the reaction temperature has a direct influence on the reaction rate. Gentric et al. [6] and [7] used the input/output linearization and optimization of the reactor temperature in order to minimize the process time and to control the polymer molecular weight.

Controlling the production rate was studied in several papers (Arzamendi and Asua [2], Gloor and Warner [8], Buruaga et al. [3], Sayer et al. [11], Zeaiter et al. [15] and Vicente et al. [13], Sheibat-Othman et al. [10]). In some of these works, the polymer properties, such as polymer molecular weight distribution and/or composition were controlled simultaneously by manipulating the feed rates of monomer(s) and chain transfer agent. In all these cases, the reaction temperature was maintained at a fixed value.

For a better control of the process productivity, the reaction temperature profile should be optimized as well as the concentration of monomer in the polymer particles. Actually, the reaction temperature affects the decomposition rate of the initiator and the propagation rate of monomer. Araujo and Giudici [1] used an iterative dynamic programming technique to minimize the reaction time and control the polymer composition by manipulating both the jacket temperature and the monomer flow rate.

Sheibat-Othman et al. [12] used input/output linearizing control to maximize the heat produced by the reaction in emulsion polymerization by manipulating both the jacket temperature and the monomer flow rate. However, the process constraints were not taken into account in the controller. In this work, the nonlinear receding horizon control, which is known to be efficient for controlling multivariables constrained nonlinear systems (Mayne et al. [9], Astorga Zaragoza [14]), is used to maximize the process productivity. The monomer flow rate and the jacket temperature are manipulated in order to do that. The process constraints, due to physical limitations such as the maximum admissible heat or the maximum possible flow rate are explicitly taken into account in the control scheme.

Since the reaction is exothermic, the calorimetry is used to estimate the heat produced by the reaction. This gives an estimate of the reaction rate. The number of moles of free monomer in the reactor and the concentration of radicals in the polymer particles can therefore be estimated [10]. Based on this information, the controller is applied to control the heat produced by the reaction.

The paper is organized as follows. First, the system model is described and the control problem is formulated in section 2. The principle of receding horizon control is briefly recalled in section 3 together with the particular formulation adopted in the present paper. In particular, the control parameterization and the definition of a modified cost function that takes into account the state constraints handling are described. Then, some validating simulations are proposed in order to assess the implementability, the efficiency and the robustness properties of the proposed feedback law. Finally, the strategy is validated experimentally in a 3 litres reactor during the polymerization of styrene .

2 Problem formulation

In order to properly state the problem under consideration, the system dynamic model is first described, then the control objective and the associated operational constraints are detailed.

2.1 The system model

A simplified model of emulsion polymerization process is given by the following four dimensional ODE's

$$\dot{N}^T = F \tag{1}$$

$$\dot{N} = F - R_p(N^T, N, T, V) \tag{2}$$

$$\dot{T} = \frac{1}{\rho_m C_p V}\Big[(-\Delta H)R_p + UA(T_j - T) + Q_{feed}\Big] \tag{3}$$

$$\dot{V} = \frac{MW_m}{\rho_m}F \tag{4}$$

Where N^T $(mole)$ is the total number of moles of monomer introduced to the reactor. N $(mole)$ is the number of residual monomer. F $(mole/s)$ is the monomer input flow rate. R_p $(mole/s)$ is the rate of transformation of monomer into polymer. T $(^o)$ is the reactor temperature. T_j (o) is the jacket temperature. V (cm^3) is the total volume of the reaction.

The reaction rate $R_p(N^T, N, T, V)$ is a state function that is given by

$$R_p = \mu \cdot V \cdot k_{p_0} e^{-EA/(RT)} \cdot M(N^T, N) \tag{5}$$

where μ is the concentration of radicals in the monomer particles, M is the concentration of monomer in the polymer particles. This latter concentration is given by :

$$M(N, N^T) = \begin{cases} \frac{(1-\phi_p^p)\rho_m}{MW_m} & \text{if} \quad \Gamma(N^T, N) \geq 0 \\ \\ \frac{N}{MW_m\left(\frac{N^T-N}{\rho_p}+\frac{N}{\rho_m}\right)} & \text{otherwise} \end{cases} \tag{6}$$

where

$$\Gamma(N^T, N) := \frac{MW_m}{\rho_m}N - \frac{1-\phi_p^p}{\phi_p^p}\Big[\frac{MW_m}{\rho_m}(N^T - N)\Big] \geq 0$$

where the following notations have been used

MW_m molecular weight of monomer

ρ_m, ρ_p monomer and polymer densities

EA the activation energy of monomer

R universal gas constant

k_{p0} pre-exponential factor

ΔH reaction enthalpy

U heat transfer coefficient

A heat transfer area between the jacket and the reactor

C_p heat capacity of the reaction medium

Q_{feed} heat exchanged with the entering components (W)

ϕ_p^p volume fraction of polymer in the polymer particles

Note that the first two equations (1)-(2) express the mass balances of N^T and N. Equation (3) is the heat transfer balance between the reactor and the jacket while the last equation (4) represents the evolution of the reaction volume due to the flow input.

Note that equations (1)-(4) give the nonlinear state space model of the polymerization reactor with the state (x) and the control vector (u) being defined as follows:

$$x := \begin{pmatrix} N^T & N & T & V \end{pmatrix} \in \mathbb{R}^4$$

$$u := \begin{pmatrix} F & T_j \end{pmatrix} \in \mathbb{R}^2$$

2.2 State measurement

In the remainder of this paper, the state represented above is assumed to be completely known. This is effectively possible according to the following scheme: The volume V and the state variable N^T are computed by integrating (4) and (1) given the input profile $F(\cdot)$ that can be measured using a balance or a flowmeter. The heat produced at some instant t, namely $Q_R(t) = (-\Delta H) \cdot R_p(t)$ is computed by calorimetry using the heat balance and the measurement of the reaction temperature T (see for example [5]). This enables $R_p(\cdot)$ to be known and hence used to estimate N by integrating equation (2)[10]. This scheme leads to measurements that can be acquired once each 10 s. It should be mentioned however that the calorimetry presents some difficulties such as the estimation of the variable heat transfer coefficient between the reactor and the jacket. For this reason, the measurement of the process state can be noisy or delayed. This consists one of the difficulties of applying the controller. Adjustment of the unknown parameters (heat transfer coefficient, heat loss) might be necessary online.

μ is also a variable parameter but is not considered as a state of the system and is not therefore taken into account in x. This is due to the fact that μ is not modelled here since it is sensitive to impurities and its model includes several other nonmeasurable states. μ is not measured but can be estimated online from the other measurements [10]. This consists another difficulty for the controller and should be kept in mind while interpreting the results.

2.3 The operational constraints

Assume that the reaction duration is t_f. In order to properly express the control objective, the operational constraints have to be clearly stated. A part of these constraints is concerned by the capacities of the pump and of the thermostated bath and another part is concerned by the operating conditions ensuring an optimal

reaction. These are the following :

(1) The maximal admissible flow rate :

$$F(\tau) \in [0, F_{max}] \quad ; \quad \forall \tau \in [0, t_f]$$

(2) The admissible range for the jacket temperature :

$$T_j(\tau) \in [T_j^{min}, T_j^{max}] \quad ; \quad \forall \tau \in [0, t_f]$$

(3) The maximal rate of variation of the control input T_j (due to thermal inertia)

$$|\dot{T}_j| \leq \dot{T}_j^{max}$$

(4) The maximal allowed heat production :

$$Q_R(\tau) := (-\Delta H) \cdot R_p(\tau) \leq Q_R^{max} \quad ; \quad \forall \tau \in [0, t_f]$$

2.4 The control objective

The control objective is to maximize the quantity of polymer produced during the reaction interval $[0, t_f]$ while respecting the operational constraints (1)-(5) defined in section 2.3. This is the same as minimizing the process time for a constant quantity of monomer to consume and also the same as maximizing the monomer conversion which is usually considered in industrial applications. This can be formally written as follows:

$$\max_{F(\cdot), T_j(\cdot)} \Big[N^T(t_f) - N(t_f) \Big] \quad \text{under (1)-(4) of section 2.3}$$

This objective has to be satisfied by a feedback design in order to be robust against model uncertainties.

3 The proposed control scheme

Since a receding horizon control scheme is adopted in the present paper, let us first of all recall the basic features underlying this principle.

3.1 Summary of receding horizon control

Receding horizon control scheme, also called predictive control, is now a widely established solution to control problems where optimal choices have to be made and where constraints are to be seriously handled. It is also a natural choice as soon as coupled multi-variable complex nonlinear systems are considered.

For a complete survey of this area, reader may consult the excellent paper [9] and the references therein. Here, only the very basic principle of receding horizon control is recalled in order to properly introduce the proposed solution to the problem at hand.

Consider a nonlinear system given by

$$\dot{x} = f(x, u) \tag{7}$$

where x is the state and u is the vector of control inputs. Assume that the control objective is expressed in terms of an optimization problem $P(x_0, T_p)$, namely

$$P(x_0, T_p) \quad :$$

$$\min_{u(\cdot) \in \mathcal{U}} J(x_0, u(\cdot), T_p) \ \text{ under } \quad \sigma(x_0, u(\cdot), T_p) \leq 0$$

where $T_p > 0$ is the prediction horizon, $\mathcal{U}$ is some subset of admissible control profiles and $\sigma(\cdot) \leq 0$ is a compact expression of the operational constraints.

The receding horizon control strategy amounts to solve at each decision instant t the optimal control problem $P(x(t), T_p(t))$ yielding the following optimal solutions

$$\hat{u}(\cdot, x(t))$$

where $\hat{u}(\cdot, x(t))$ is the optimal control profile defined on the time interval $[t, t + T_p(t)]$ and to apply the first *portion* of the optimal profile over $[t, t + dt]$. At the next decision instant $t + dt$, the new optimal control problem $P(x(t + dt), T_p(t + dt))$ is solved yielding the optimal solutions

$$\hat{u}(\cdot, x(t + dt))$$

and the first portion of $\hat{u}(\cdot, x(t + dt))$ is applied over $[t + dt, t + 2dt]$. The procedure is then repeated indefinitely for classical systems or until the end of the batch operation for batch reactors.

Now $P(x(t), T_p(t))$ is rigorously an infinite dimensional optimization problem since $u(\cdot)$ needs an infinite number of degrees of freedom to be completely defined. That is the reason why a finite dimensional parametrization of the open loop profiles used in the definition of $P(x, T_p)$ is needed. The family of piece wise constant control profiles given some sampling period $\tau_s > 0$ is a conceptually easy way to achieve this objective, however, this choice may lead to a rather high dimensional optimization problem that may be difficult to solve in a reasonable time.

In the following section, the particular parametrization used to define the control profiles $F(\cdot)$ and $T_j(\cdot)$ is presented.

3.2 The control parametrization

The control parametrization used in the present paper for the control inputs T_j and F are depicted on Fig. 1 and Fig. 2 respectively. More precisely, the admissible profiles for T_j over some time interval $[0, t_f]$ are given by the following three dimensional parametrization with the parameter vector given by (w_1, w_2, t_1) :

$$T_j(t) = Sat_{T_j^{min}}^{T_j^{max}} \Big(T_j(0) + \int_0^t w(\tau) d\tau \Big) \tag{8}$$

$$w(t) := \begin{cases} w_1 & \text{if} \quad t < t_1 \quad t_1 \in [0, t_f] \\ w_2 & \text{if} \quad t \in [t_1, t_f] \end{cases} \tag{9}$$

where w_1 and w_2 are restricted to $[-\dot{T}_j^{max}, \dot{T}_j^{max}]$ in order to meet the constraint (3) of section 2.3 while the constraint (2) is structurally imposed by the use of the saturation function in equation (8).

The parametrization of the input flow rate F over a time interval $[0, t_f]$ is given by (see Fig. 2) :

$$F(t) = F(0) + (F^f - F(0))[1 - e^{-\lambda t}] \tag{10}$$

this is a scalar parametrization with the only parameter $F^f \in [0, F_{max}]$ enabling the constraint (1) of section 2.3

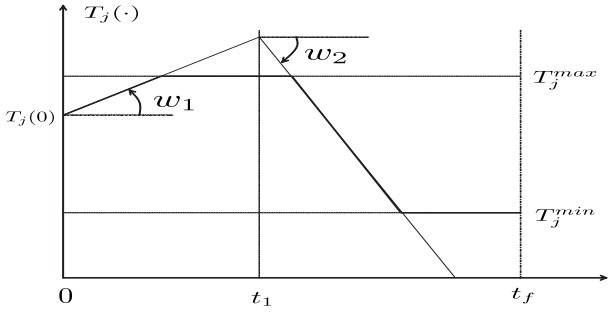

Fig. 1. Parametrization of the control input $T_j(\cdot)$ over a time interval $[0, t_f]$. This parametrization is used in the definition of the receding horizon control formulation. $T_j(\cdot)$ is defined by three parameters: the two slopes w_1 and w_2 that have to belong to the admissible range $[-\dot{T}_j^{max}, \dot{T}_j^{max}]$ and the switching time $t_1 \in [0, t_f]$.

to be structurally satisfied.

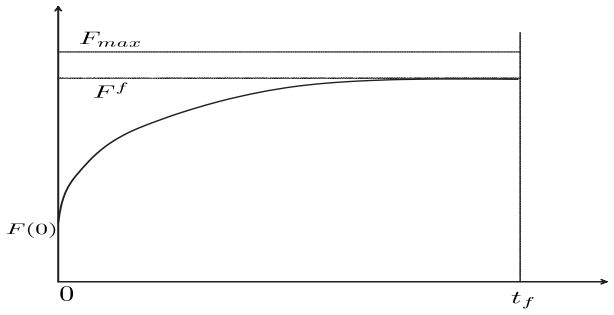

Fig. 2. Parametrization of the control input $F(\cdot)$ over a time interval $[0, t_f]$. This parametrization is used in the definition of the receding horizon control formulation. $F(\cdot)$ is defined by one parameter, namely its asymptotic value F^f.

To summarize, the control input parametrization is defined over a time interval $[0, t_f]$ by the following four dimensional parameter vector

$$p := \begin{pmatrix} w_1/\dot{T}_j^{max} \\ w_2/\dot{T}_j^{max} \\ t_1/t_f \\ F^f/F_{max} \end{pmatrix} \in \mathcal{P} := [-1, 1]^2 \times [0, 1]^2 \qquad (11)$$

This control parametrization structurally leads to the satisfaction of the operational constraints (1)-(3) of section 2.3. The satisfaction of the remaining constraint (4) of section 2.3 is guaranteed by a suitable modification of the cost function. This is explained in the following section.

In the remainder of this paper, the control profile $T_j(\cdot)$ and $F(\cdot)$ associated to a particular choices of t_f and $p \in \mathcal{P}$ are denoted as follows

$$T_j(\cdot, p, t_f) \quad ; \quad F(\cdot, p, t_f)$$

3.3 The modified cost function

Assume that the reaction takes place during T_{batch} units of time. Assume some instant $t \in [0, T_{batch}]$. The prediction horizon at that instant is then given by :

$$T_p(t) = T_{batch} - t \qquad (12)$$

Each choice of the control parametrization $p \in \mathcal{P}$ results in the following two open-loop control profiles over

$[t, T_{batch}]$,

$$T_j(\cdot, p, T_p(t)) \quad ; \quad F(\cdot, p, T_p(t)) \tag{13}$$

The modified cost function at instant t is given by :

$$J(p,t) = \left[1 - \frac{1}{\varepsilon}\max\Big(0, \sup_{\tau\in[t,T_{batch}]} \frac{Q_R(\tau,p) - Q_R^{max}}{Q_R^{max}}\Big)\right] \times \left[N(T_{batch},p) - N^T(T_{batch},p)\right] \tag{14}$$

where $Q_R(\cdot,p)$, $N(\cdot,p)$ and $N^T(\cdot,p)$ are the predicted values given the initial state $x(t)$ and the control profiles (13) that would be used on $[t, T_{batch}]$. $\varepsilon > 0$ is a small parameter.

The relevance of the cost function (14) is shown by the following result :

Proposition 1 Provided *that there exist admissible control profiles over* $[t, T_{batch}]$ *that lead to the satisfaction of constraint* $Q_R(\tau) \leq Q_R^{max}$ *over* $[t, T_{batch}]$*, a parameter vector* $\hat{p}(x(t), T_p(t))$ *that minimizes* $J(p,t)$ *leads to state trajectories satisfying*

$$Q_R(\tau) \leq (1+\varepsilon) Q_R^{max} \tag{15}$$

for all $\tau \in [t, T_{batch}]$

In other words, proposition 1 states that whenever there are solutions that respect the constraint (4) of section 2.3, the modified cost function (14) leads to trajectories that do not violate this constraint by more than $\varepsilon\%$.

Proof

This comes from the fact that if p_1 is an admissible parametrization that meets the constraint, then one has

$$J(p_1,t) = N(T_{batch},p_1) - N^T(T_{batch},p_1) < 0 \tag{16}$$

(such p_1 exists by assumption). This is because for such p_1, one has

$$\sup_{\tau\in[t,T_{batch}]} \frac{Q_R(\tau,p_1) - Q_R^{max}}{Q_R^{max}} \leq 0$$

and therefore

$$\max\Big(0, \sup_{\tau\in[t,T_{batch}]} \frac{Q_R(\tau,p_1) - Q_R^{max}}{Q_R^{max}}\Big) = 0$$

Now let p^* be a solution that violates the constraint by more than $\varepsilon\%$, this means that

$$\sup_{\tau\in[t,T_{batch}]} \frac{Q_R(\tau,p^*) - Q_R^{max}}{Q_R^{max}} > \varepsilon$$

and hence

$$1 - \frac{1}{\varepsilon}\max\Big(0, \sup_{\tau\in[t,T_{batch}]} \frac{Q_R(\tau,p^*) - Q_R^{max}}{Q_R^{max}}\Big) \leq 0 \tag{17}$$

and since $N(T_{batch},p^*) - N^T(T_{batch},p^*) < 0$, equation (17) implies that

$$J(p^*,t) \geq 0 > J(p_1,t)$$

which indicates that p^* is not an optimal solution as soon as it violates the constraint by more than $\varepsilon\%$. This ends the proof. ♢

3.4 The receding horizon feedback

Let $\tau_s > 0$ be some sampling period for control. The instants $(k\tau_s)_{k\geq 0}$ becomes the decision instants where

the optimization problems $P(x(k\tau_s), T_p(k\tau_s))$ are solved in order to update the control inputs to apply to the system on $[k\tau_s, (k+1)\tau_s]$. More precisely, let $\hat{p}(k\tau_s)$ be given by :

$$\hat{p}(k\tau_s) := Arg \quad \min_{p\in\mathcal{P}} J(p, k\tau_s) \tag{18}$$

the receding horizon control scheme amounts to apply the following control over the sampling period $[k\tau_s, (k+1)\tau_s]$:

$$T_j(k\tau_s + \tau) := T_j(\tau, \hat{p}(k\tau_s), T_p(k\tau_s)) \quad \forall \tau \in [0, \tau_s] \tag{19}$$

$$F(k\tau_s + \tau) := F(\tau, \hat{p}(k\tau_s), T_p(k\tau_s)) \quad \forall \tau \in [0, \tau_s] \tag{20}$$

where $T_p(t)$ is given by (12).

4 Simulation results

In this section, simulation of the closed loop system's performance under the proposed constrained receding horizon control are proposed to assess the efficiency and the robustness of the proposed feedback controller. Two sets of simulations are proposed illustrating the behavior under nominal conditions and under realistic system's uncertainties. The execution times necessary to solve the associated optimization problem are reported proving the real time implementability of the proposed scheme. The parameters of the polymerization of styrene are used in the simulations. These are given on table 1.

The computations are done using FORTRAN source code on a 1.3 GHz Pentium-III PC. The optimization has been done using the optimization subroutine BCPOL of the numerical library IMSL. The maximum number of function evaluation has been taken equal to 100.

Parameter	Value	Unit
C_p	1714	(J/Kg/K)
UA	6	$(J/K/s)$
T_{feed}	25	(K)
ρ_m	0.904	(kg/cm^3)
ϕ_p^p	0.4	–
k_{p0}	1.05×10^{10}	$(cm^3/mol/s)$
EA	2.9544×10^4	(J/mol)
$(-\Delta H)$	71060	(J/mol)
C_{Pfeed}	1714	(J/Kg/K)
MW_m	104.15	(g/mol)
ρ_p	1.04	(kg/cm^3)
N_p	10^{17}	–
$\bar{n}$	0.5	–
F^{max}	10^{-3}	(mol/s)

Table 1

Parameter values of the polymerization reactor

A sampling period $\tau_s = 60\ s$ has been used. In the definition of the admissible profile for F [see equation (10)], the value $\lambda = \frac{3}{10}\ s^{-1}$ has been used. Note that a sampling period of 10s can be implemented experimentally.

4.1 Nominal case

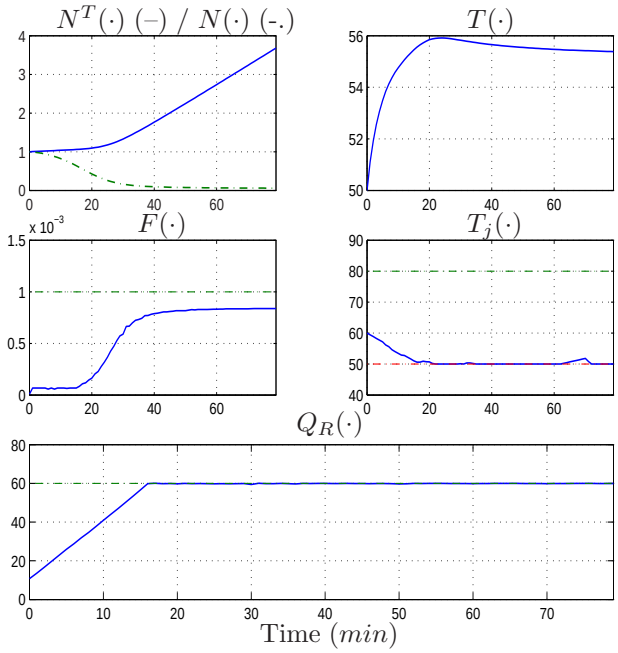

Fig. 3. Behavior of the closed loop system under the receding horizon feedback. $Q_R^{max} = 60$, $T_j^{max} = 80^o$, $T_j^{min} = 50^o$, $F_max = 0.001\ mol/s$. $\lambda = 1/10s^{-1}$. Sampling period $\tau_s = 1\ min$. $\varepsilon = 0.05$. Initial conditions $N(0) = N^T(0) = 1$, $T = 50^o$, $V(0) = 2$

Fig. 3 shows the behavior of the closed loop system under the proposed receding horizon feedback with the upper bound Q_R^{max} taken equal to 60.

Note how the controller steers the heat production Q_R to its maximum admissible value and maintain it at that level in order to maximize the production rate (recall that $Q_R = (-\Delta H) \cdot R_p$ and that R_p is nothing but the production rate).

In order to assess the multivariable character of the proposed feedback and the quality of the constraint handling, Fig. 4 shows the behavior of the closed loop system when the the maximal flow rate F_{max} is decreased to 0.0008 rather than 0.001. Note how in this case, contrary to the preceding scenario where the temperature approaches its minimal value (50^o), the controller in Fig. 4 uses the temperature jacket to realize the control objective (Remaining close to the maximal value $Q_R^{max} = 60$). This leads to the two control inputs being saturated by their maximal values.

Note also that it is rigorously impossible to stay exactly at the maximal level $Q_R^{max} = 60$ because of the saturation on the control inputs. The controller stabilizes Q_R to the maximal possible value.

Fig. 5 shows the evolution of the control parametrization p (see section 3.2) during the reaction depicted in Fig. 4. Recall that the first three parameters concern the definition of the open loop profiles for the jacket temperature T_j while the last one defines the open loop profile of F.

4.2 Robustness against model uncertainties

Very often, model uncertainties are due to the presence of complex phenomenon that are difficult to model by explicit mathematical framework. This is the case for instance when the evolution of the concentration of radicals μ is considered. Recall that μ appears in the very definition (5) of the reaction rate R_p. This parameter is

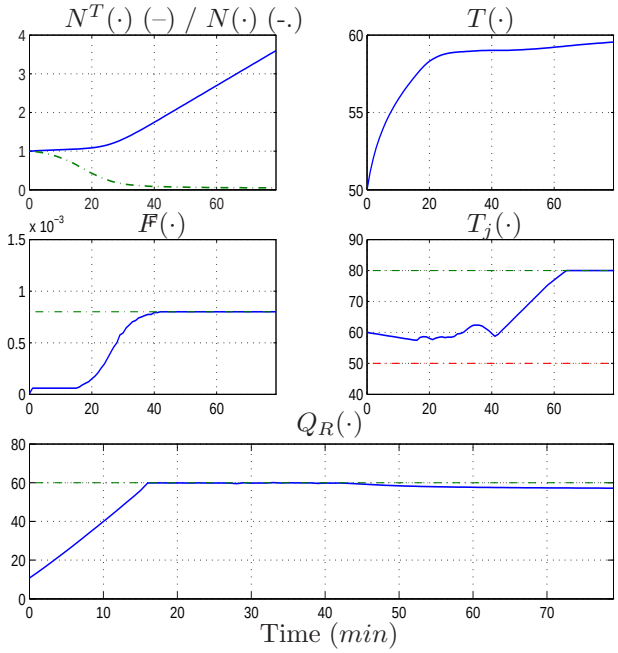

Fig. 4. Behavior of the closed loop system under the same conditions as Fig. 3 with a lower maximal allowable flow rate $F_{max} = 0.0008$. Note how the controller saturates the two control inputs in order to meet the achieve the control objective (remain close to the maximal allowable heat production $Q_R^{max} = 60$.

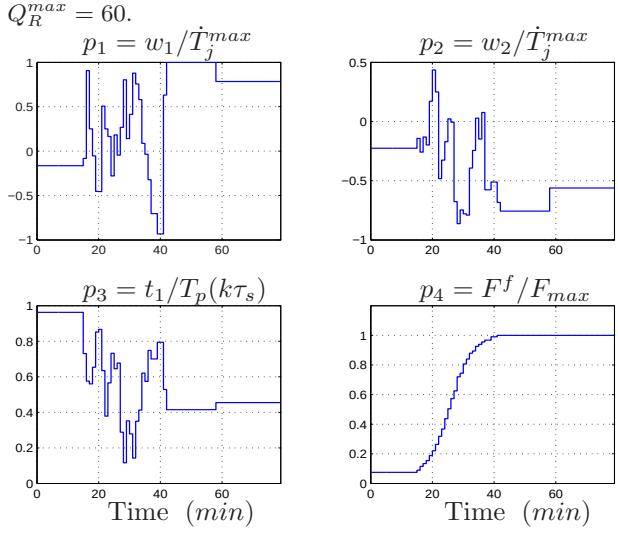

Fig. 5. Evolution of the optimal parameter vector $\hat{p}(k\tau_s) \in \mathcal{P} \in [-1,1]^2 \times [0,1]^2$ during the batch depicted on Fig. 4.

not modelled here and therefore the controller assumes it is constant in the prediction scheme. However,μ might change with time as a function of temperature or concentration of monomer. It should be necessary therefore to test the robustness of the controller against high variation of μ with time.

In order to do so, the following model is used for $\mu(t)$ during the reaction (note that this model is not known by the controller that only measures the value of μ at each sampling instant) :

$$\mu(t) = \left[1 + \frac{\psi_f \cdot t}{T_{batch}}\right] \cdot \mu_{nom} \quad ; \quad \mu_{nom} := \frac{\bar{n} \cdot N_p}{N_A} \qquad (21)$$

More clearly, if $\psi_f = 0$ then no variation of μ with time is considered (μ is constant); for $\psi_f \neq 0$, the value of μ linearly increases during the reaction from μ_{nom} to $(1 + \psi_f) \cdot \mu_{nom}$. In both cases, the evolution of μ is not known by the controller. In the first case, with no variation of μ with time, the controller acts well, as shown in the first simulation (Fig. 3.

Fig. 6 shows the behavior of the closed loop system for $\psi_f = 2$. Note that the controller avoids constraint violation (by more than 5%) despite the fact that μ is multiplied by 3 ($\psi_f = 2$) during the reaction duration. During a sampling time, the controller switches off temporarily the flow rate in order to avoid constraint violation on the allowed heat production Q_R.

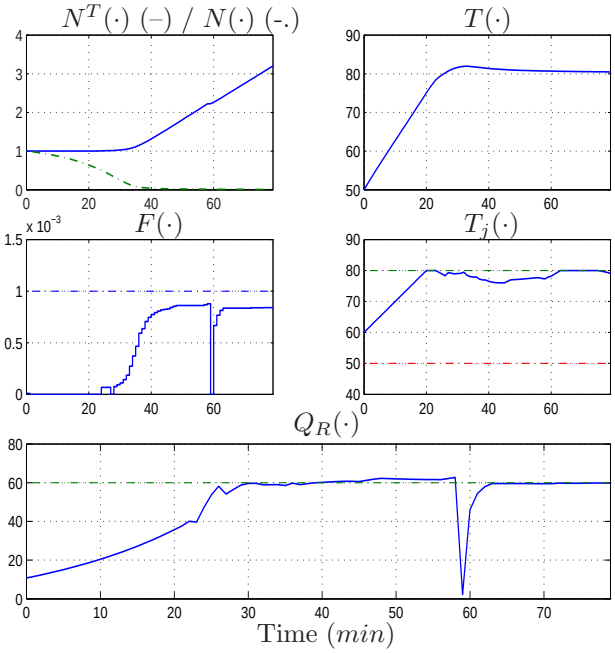

Fig. 6. Behavior of the closed loop system under the same conditions as Fig. 3 with the model uncertainty on the concentration of radicals given by (21). Case where $\psi_f = 2$, namely, the value of μ in (5) increases linearly from μ_{nom} to $3 \cdot \mu_{nom}$ during the reaction time interval $[0, T_{batch}]$. The dynamics of μ is unknown to the controller but current values are accessible to measurement according to section 2.2. Note how the controller switches off temporarily the input flow rate in order to avoid constraint violation on the heat production Q_R.

5 Experimental results

5.1 Process monitoring

The polymerization reactions are known to be exothermic and are therefore usually monitored by calorimetry. The reactor and jacket temperatures are measured online. The unknown terms in the heat balance (Qloss and U) can be estimated by correlation to the solid contents (Fevotte et al. [5], Buruaga et al. [3]) which requires measuring the solid contents during the reaction at discrete intervals. In this work, the heat transfer coefficient and the heat loss were found to be constant during the reaction. Therefore, these coefficients were identified before the reaction and the obtained values were introduced in the heat balance to estimate the heat produced by the reaction. The monomer conversion was then estimated from the heat balance. This allows the estimation of the number of moles of monomer and the concentration of radicals in the reactor using for example a Kalman filter (Fan and Alpay [4]) or a high gain observer (Sheibat-Othman et al. [10]).

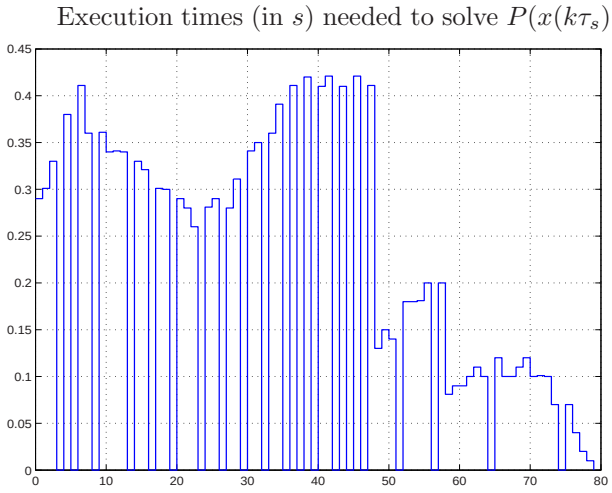

Fig. 7. The computation times needed to solve the four dimensional optimization problem at each sampling instant of the scenario depicted in Fig. 6. The upper bound of the execution times (say 0.5 s) is to be compared to the sampling period $\tau_s = 60$ s

5.2 Experimental set-up

The controller was validated experimentally on a 3 litres jacketed reactor. The reactor is equipped with a stirrer

with a stirring rate of 200 rpm which ensures the homogeneity of the reactor temperature. The cover of the reactor is equipped with a condenser to cool the evaporating components. Temperatures are measured in the reactor, at the inlet and at the outlet of the jacket using PT100 probes. These data are acquired every 10s. A controlled pump allows the introduction of monomer. The exact amount introduced into the reactor is measured using a balance where the masse is registered every 10s. A local PID controller is therefore implemented to control the pump. This controller takes its set-point from the nonlinear predictive controller. The jacket temperature is controlled using a cryothermostat batch were the maximum heating or cooling rates are identical (1.5C/min).

5.3 Experimental validation

Styrene was used for the experimental validation of the controller. The used recipe is given in table 2.

	Initial charge (g)	Feed
Styrene	145	1000
Dodecyl sulfate, sodium salt	4	8
Potassium persulfate	4	–
H2O	1000	500

Table 2

Recipe used for the experimental validation of the controller

The desired heat produced by the reaction was set to 60W. The maximum number of function evaluation in the controller has been taken equal to 150 in this experiment. Fig. 8 shows the evolution of Q_R during this experiment. No attempt was done to accelerate the convergence time to the set-point by increasing the reaction temperature during the first 15 minutes in order to anticipate the important heat generated by the nucleation taking place at the beginning of the reaction. The jacket temperature was therefore fixed at $60C$ during this time (Fig. 9). By the same way, the monomer flow rate (Fig. 10) was fixed at 0 when $\Gamma(N^T, N) = 0$ which means that the polymer particles are saturated with monomer (Fig. 11). This corresponds to the first 20 minutes of the reaction. Fig. 11 shows both the desired monomer flow rate calculated by the controller and the real one obtained experimentally while coupled with the local controller. The local controller generates small oscillations since it uses the flow rate generated by deriving the mass obtained from the balance. However, the desired flow rate calculated by the receding horizon controller does not oscillate which means that the nonlinear controller is well tuned. These oscillations affect the heat produced by the reaction as shown on Fig. 8. Fig. 8 shows that Q_R presents also some important oscillations that are not due to the fluctuations in the flow rate of monomer but to an important unpredicted change in the reaction rate. Fig. 12 shows the profile of μ that is proportional to the reaction rate. It is important to remind here that the dynamic of μ is not predicted by the controller as it is estimated online. A constant value of μ is used in the controller during the prediction. For example at 130

minutes a very important variation of μ was observed. This occurs if a gel effect takes place in the polymer particles which decreases the termination rate of radicals and causes an important increase in μ. Nucleation of new particles also causes an increase in the reaction rate. However, the concentration of monomer in the polymer particles was very low and therefore we exclude the possibility of new nucleation. It can be seen however that even with very important variation in the process dynamic, the controller could decreases Q_R rapidly. This phenomena can perhaps be improved by including an estimate of μ in the prediction scheme.

This experiment shows that even if the process model seems simple its dynamic can change rapidly in an unpredicted way.

Compared to the input/output linearizing control used by Sheibat-Othman et al. [12], the predictive controller shows some advantages. First of all, the process constraints are included in the control scheme in this work. Second, the controller was also found to stabilize rapidly the system. No filters on the desired trajectories were necessary to stabilize the controller as was found in [10]. Third, the predictive controller gives an optimal trajectory of the inputs on the optimization horizon while the input/output linearizing control gives the inputs to imply at that time. The prediction horizon was taken to be the whole reaction time in the studied simulations and experimentally. Therefore a fixed horizon was implemented. This was possible since the reaction time was not very important which allows to realize the optimization online. For longer reaction times such as continuous reactions, it would be interesting to consider a receding horizon on one to two hours for example.

It should be mentioned however that input-output linearizing control can be calculated quasi instantaneously while the receding horizon control depends on the number of iterations fixed in order to find the optimal solution.

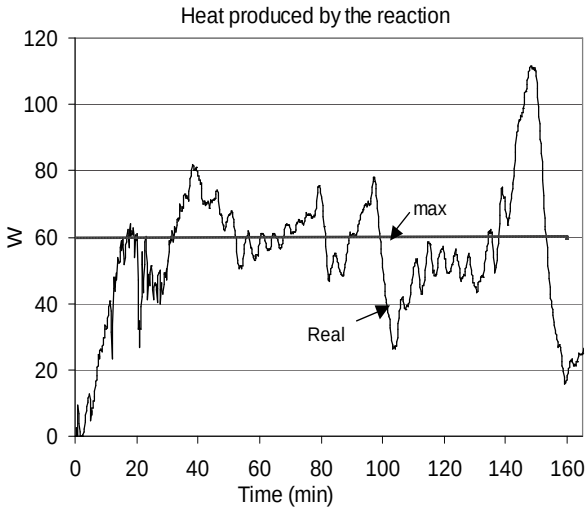

Fig. 8. Experimental validation of the controller. The heat produced by the reaction with a maximal constraint at 60 W

6 Conclusion and future work

In this paper, a multi-variable constrained receding horizon control scheme has been proposed to maximize the production during polymerization reactions. Two control inputs are used: the inlet flow rate and the jacket temperature. A key feature of the proposed scheme is the very simple control parametrization enabling a real

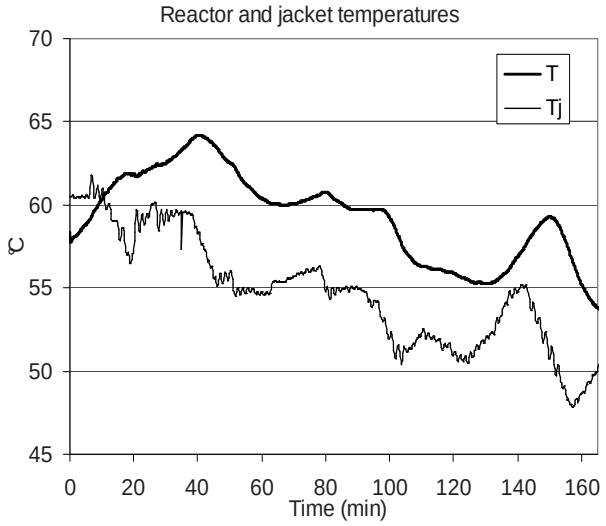

Fig. 9. Experimental validation of the controller. Reactor and jacket temperatures

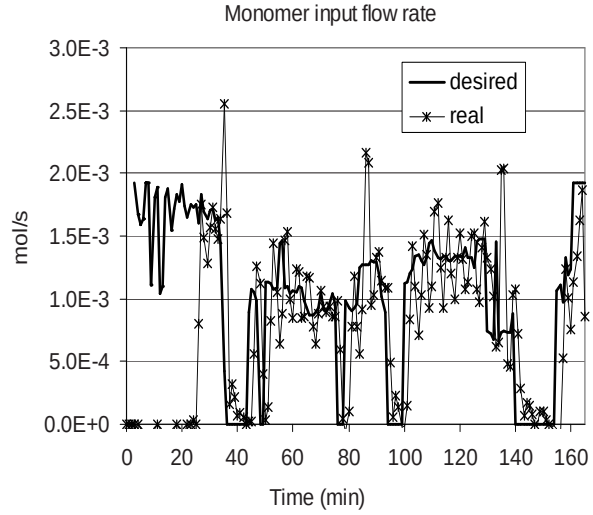

Fig. 10. Experimental validation of the controller. Controlled monomer flow rate and the reaction rate

time implementability of the proposed scheme despite the relatively low sampling time (60 s). Another interesting feature is the explicit handling of all operational constraints that would be difficult to be rigorously handled by more classical schemes.

Investigations also showed nice robustness properties

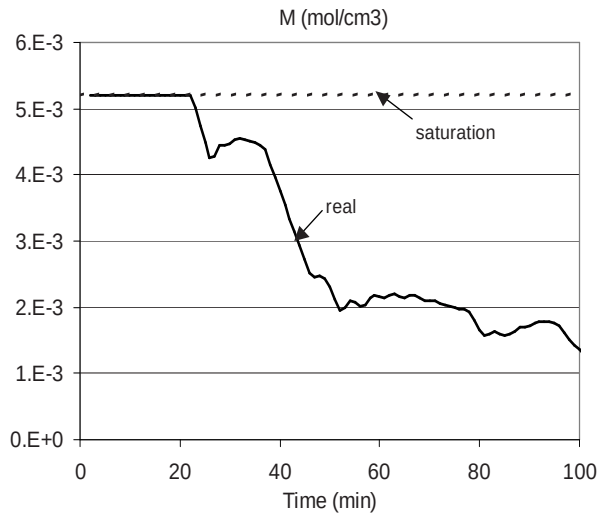

Fig. 11. Experimental validation of the controller. Concentration of monomer in the polymer particles

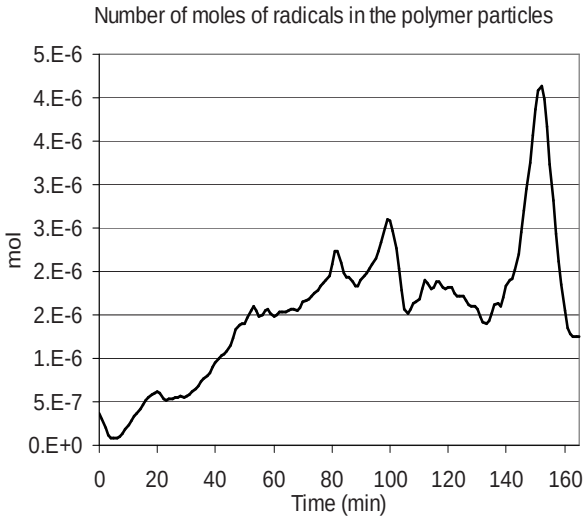

Fig. 12. Experimental validation of the controller. Number of moles of radicals in the polymer particles (μ)

against unmodeled dynamics like the one affecting the concentration of radicals in the polymer particles that generally increases during the reaction due to the gel effect following very complex and unpredictable laws.

Note finally that the computation times needed to solve the optimization problem are even compatible with a

higher measurement acquisition frequency (say 0.1 Hz) that is practically feasible. This leads to more reactive controller that would certainly make the results even better than it appears from the simulations proposed in this paper.

The controller also gave good results while implemented experimentally. It could be seen that even with a highly varying non modelled state, the controller could bring back the system to the set-point without hight oscillations.

References

[1] P.H.H. Araujo and R. Giudici. Optimization of semicontinuous emulsion polymerization reactions by idp procedure with variable time intervals. Computers and Chemical Engineering, 27:1345–1360, 2003.

[2] G. Arzamendi and J. Asua. Copolymer composition control of emulsion copolymer in reactors with limited capacity for heat removal. Industrial Engineering Chemistry, 30:1342–1350, 1991.

[3] I. S. Buruaga, Ph. D. Armitage, J. R. Leiza, and J. M. Asua. Nonlinear control for maximum production rate latexes of well-defined polymer composition. Ind. Eng. Chem. Res., 36:4243–4254, 1997.

[4] Sh. Fan and Estat Alpay. Calorimetric estimation for a batch-loop emulsion polymerization reactor. Chemical Engineering Science, 59:2811–2815, 2004.

[5] G. Fevotte, I. Barudio, and J. Guillot. An adaptive inferential measurement strategy for online monitoring of conversion in polymerization processes. Thermochimica Acta, 289:223–242, 1996.

[6] C. Gentric, F. Pla, and J.P. Corriou. Experimental study of the nonlinear geometric control of a batch emulsion polymerization reactor. Computer Chemical Engineering, 21:S1043–S1048, 1997.

[7] C. Gentric, F. Pla, M.A. Latifi, and J.P. Corriou. Optimization and non-linear control of a batch emulsion polymerization reactor. Chemical Engineering Journal, 75:31–46, 1999.

[8] P. E. Gloor and R.J. Warner. Developing feed policies to maximize productivity in polymerization process. Thermochimica Acat, 289(2):243–265, 1996.

[9] D. Q. Mayne, J. B. Rawlings, C. V. Rao, and P. O. Scokaert. Constrained model predictive control: Stability and optimality. *Automatica*, 36:789–814, 2000.

[10] N. Sheibat Othman, G. Fevotte, and T. F. McKenna. Biobjective control of emulsion polymerizations: control of the polymer composition and the concentration of monomer in the polymer particles. Chemical Engineering Journal, 98:69–79, 2004.

[11] C. Sayer, G. Arzamendi, J.M. Asua, E.L. Lima, and J.C. Pinto. Dynamic optimization of semicontinuous emulsion copolymerization reactions: composition and molecular weight distribution. Computers and Chemical Engineering, 25:839–849, 2001.

[12] N. Sheibat-Othman and S. Othman. Control of and emulsion polymerization reactor. Ind. Eng. Chem. Res., 45:206–211, 2006.

[13] M. Vicente, J.R. Leiza, and J.M. Asua. Maximizing production and polymer quality (MWD and composition) in emulsion polymerization reactors with limited capacity of heat removal. Chemical Engineering Science, 58:215–222, 2003.

[14] C.M. Astorga Zaragoza, S. Othman, and H. Hammouri.

Moving horizon control of a dentrification reactor. WSES/ International Conferences AMTA 2000- MCBC 2000-MCBE 2000 JAMAICA, pages 931–936, 2000.

[15] J. Zeaiter, J. A. Romagnoli, G. W. Barton, V. G. Gomes, B. S. Hawkett, and R. G. Gilbert. Operation of semi-batch emulsion polymerization reactors: Modeling, validation and effect of operating conditions. Chemical Engineering Science, 57:2955–2969, 2002.